Large Scale Commercial Fabrication of High Quality Graphene-Based Assays for Biomolecule Detection

Mitchell B. Lerner1, Deng Pan2,3, Yingning Gao1, Lauren E. Locascio2, Kian-Yong Lee4, Jolie Nokes2, Savannah Afsahi2, Jeremy D. Lerner1, Amy Walker2, Philip G. Collins3, Karen Oegema4, Francie Barron2, Brett R. Goldsmith2

[1]Production Division, Nanomedical Diagnostics Inc., San Diego, CA 92121 USA
[2]Research and Development Division, Nanomedical Diagnostics Inc., San Diego, CA 92121 USA
[3]Department of Physics and Astronomy, University of California, Irvine, CA 92697 USA
[4]Ludwig Institute for Cancer Research, San Diego, CA 92093, USA

This is a pre-print of a paper that has been published in a scientific journal:

Lerner, *et. al*., Large Scale Commercial Fabrication of High Quality Graphene-Based Assays for Biomolecule Detection, Sensors & Actuators B (2016), DOI: 10.1016/j.snb.2016.09.137

ABSTRACT

Large numbers of high quality graphene transistors with mobility approximately 5000 $cm^2/V*s$ were fabricated by chemical vapor deposition and packaged into ceramic carriers with an open cavity design. The ceramic carrier is compatible with standard electronics assembly, enabling the readout of graphene properties on the benchtop without large, expensive probing systems. After chemical functionalization, these sensors demonstrate sensitivity in the pM range and selectivity to many classes of biomolecules as a three terminal liquid-gated field effect transistor. High precision measurements of protein kinetics captured using this technology, commercially known as Agile R100, are comparable and can exceed the capabilities of state-of-the-art biomolecule characterization tools.

INTRODUCTION

The tools of immunological research have not advanced significantly in decades.[1–3] Monoclonal and polyclonal antibodies remain at the heart of the pursuit, while new kits and assays make modest improvements on signal transduction for specific applications.[4] New technologies are emerging to displace the workhorse ELISAs and Western blots, but there are still large gaps in the biotechnology space for generalized protein binding quantification and dynamic binding kinetics.[5,6] Graphene, a two dimensional sheet of hexagonally arranged carbon atoms, has been touted as a wonder material since its isolation in 2004.[7,8] With the highest room temperature mobility of any material, graphene is extremely attractive for semiconductor devices such as radio frequency and digital transistors.[9] As a 2-dimensional material, every atom in a graphene sheet is in direct contact with its environment, making it an ideal candidate for sensing applications.[10] Indeed, graphene has been incorporated into sensors of all varieties, including pressure sensors,[11] vapor sensors,[12,13] optical sensors,[14] and biomolecular sensors.[15]

However, while these proof of concept studies are highly compelling, the launch of graphene devices as part of a commercial product has been met with challenges on several fronts.[16] First, synthesizing electronics quality graphene reproducibly in large quantities has been heavily investigated, with the most cost effective method being chemical vapor deposition (CVD) of graphene from a carbon feedstock gas at high temperatures.[17,18] Several reports describe the production of graphene via roll to roll processing for touch screen applications, and some companies have launched sales of graphene-enabled cell phone touchscreens.[18–20] The second hurdle in graphene manufacturing is removing the graphene from its growth substrate and transferring it to the target substrate, often a silicon wafer. Several nondestructive, low contamination solutions are available, including thermal release tape, pressure sensitive adhesives, and bubbling transfer.[21,22] The final and most neglected of large scale graphene device adoption challenges is integration with conventional electronic measurement systems, which is critical since it is infeasible to require every potential user to have a semiconductor parameter analyzer readily available.[23,24] In order to ensure that graphene maximizes its utility as the disruptive sensor technology that it can be, all of these difficulties must be surmounted. In this paper, we describe a set of manufacturing techniques that addresses each aspect of graphene incorporation into a highly sensitive, selective, and versatile biosensor chip called the Agile (Automatic Graphene ImmunoLinked Electronic) sensor. This system has recently been used for advanced protein characterization in a peer-

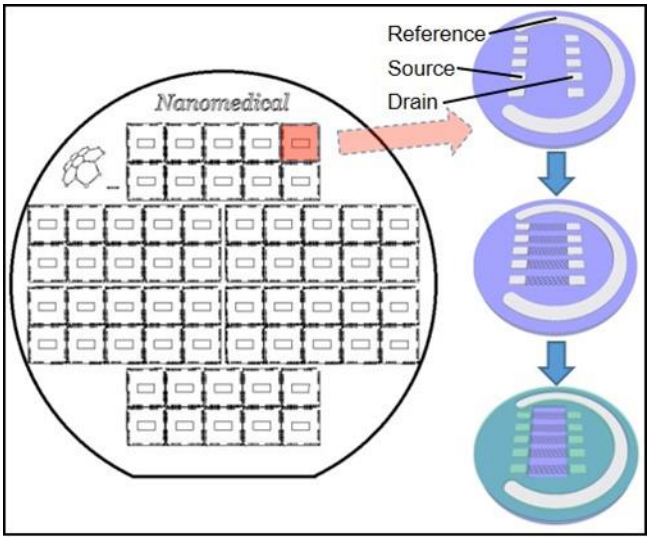

Figure 1: Wafer level graphene transistor fabrication process flow. Ti/Pt source, drain, and reference electrodes are patterned, followed by graphene deposition and etching. Finally, oxide is deposited and etched to reveal the graphene channels.

reviewed study by an independent research group.[25] Though graphene-enabled sensors were predicted to hit the market after 2025, Agile technology is available today, nearly a decade ahead of the expected state of the art.[26,27]

EXPERIMENTAL SETUP AND FABRICATION

Chips are fabricated at a commercial MEMS foundry in several stages using conventional processing techniques. Ti/Pt source, drain, and reference electrodes with corresponding bond pads are patterned on 4" silicon wafers using a liftoff process. Wafers are then cleaned by piranha etching to remove all potential organic residues that could act as dopants of the final graphene devices. Concurrently with the electrode patterning, high quality graphene films are grown in tube furnaces at temperatures exceeding 1030°C on copper foil (Alfa Aesar Item #46365) by catalytic decomposition of methane gas as reported in the literature.[28] Graphene films are spin coated with a PMMA support layer (MicroChem PMMA C4 950), then delaminated from the copper foil growth substrate by bubbling transfer as described in the literature.[29] The graphene films are deposited on top of the electrode-patterned wafers and thoroughly cleaned with acetone and isopropanol and a forming gas anneal at 200°C for 1 hour. The final fabrication stage consists of patterning the graphene sheets into defined channels between the source-drain electrodes and then passivating the Ti/Pt electrodes with a plasma-enhanced CVD silicon oxide layer deposited over the entire wafer. Finally, the graphene channels are released using reactive ion etching. The process flow is depicted in Figure 1. Given the geometry of the graphene channels, a device with resistance of 2 - 50 kΩ is considered acceptable for further processing. Two terminal electrical resistance characterization at this stage of fabrication indicates a yield of >98% of functional graphene devices across thousands of devices tested.

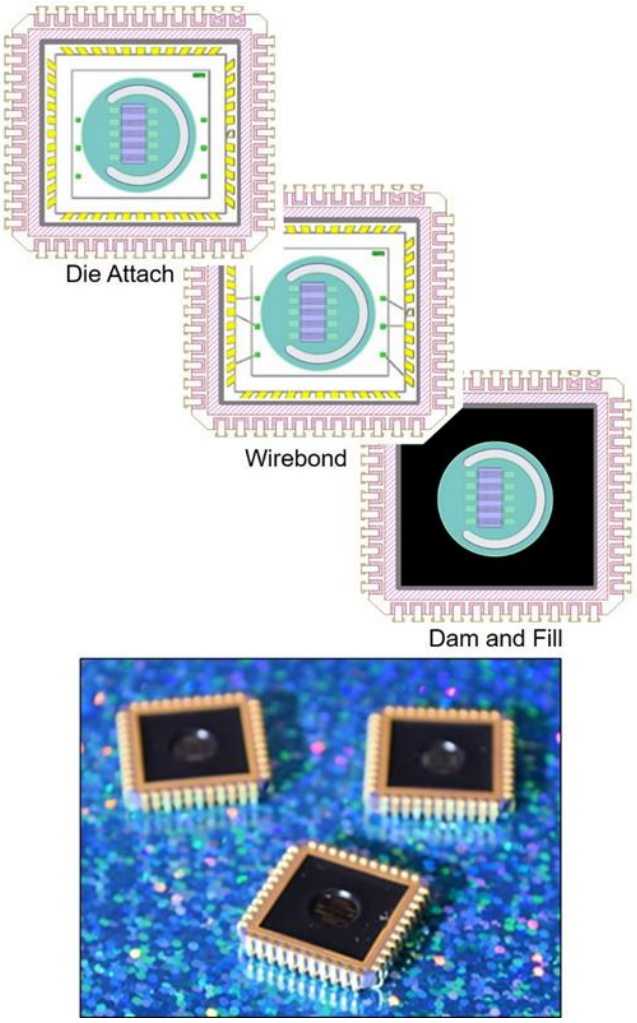

Figure 2: Chip packaging consists of die attach into a 44 pin CQFJ package, followed by Au ball wire bonding and lastly dam and encapsulation using a heat cured epoxy. Several completed Agile chips are depicted with the open cavity available for liquid biological sample insertion.

While much attention has been paid to graphene growth and transfer, relatively little effort has been spent on graphene-compatible electronics packaging.[23,24] For widespread adoption of graphene-enabled hardware, the technology must operate in a form factor compatible with common laboratory infrastructure. Our graphene wafers are first diced into 9 mm x 9 mm die. Each die is attached to a 44 pin ceramic quad flat J lead (CQFJ) package (Kyocera Part #PB-F87049) using epoxy and wire bonded to the package. The wire bonds are encapsulated in epoxy using a dam and fill process, leaving an open cavity over the exposed graphene channels for biological sample placement as depicted in Figure 2. The entire package is annealed at 200°C in forming gas (95% Ar/5% H_2) to remove any potential residues from the packaging process. Another set of resistance characterization measurements on thousands of devices indicate yield of greater than 90% at this stage. This completes the fabrication of the three terminal graphene field effect transistor (FET) with the on-chip Pt pseudo-reference

Figure 3: A complete prototype Agile R100 measurement system, including reader hardware (black box), cartridge, and chip, which is USB-compatible in a small form factor.

electrodes serving as a liquid gate through the conductive solution containing the biologic being measured.

Packaged chips fit into standard sockets for the 44 pin CQFJ package (Assmann Part # A-CCS-028-Z-T), which are loaded onto printed circuit boards. Each circuit board connects to specially designed measurement hardware from Varasco Engineering consisting of a current amplifier, picoammeter, switching matrix, analog voltage supply, analog to digital converter, and microprocessor controller in one unit. This chip reader then connects to any computer via USB. The reader hardware is capable of delivering two analog voltages between +/- 255 mV with a resolution of 1 mV using a 24 bit analog to digital converter with a programmable sample rate from 7 Hz to 3500 Hz. The current measurement has a linear range of 10 nA to 200 uA with an rms noise floor of 30 pA. The entire system, including the chip, the socket, and the reader hardware, weighs less than 1 kg and is roughly the size of a large cell phone (Figure 3).

RESULTS AND DISCUSSION

Electronic Transport of Large Scale Graphene Transistor Arrays

The electronic transport properties of 12,792 graphene transistors obtained from the reader hardware are depicted in Figures 4 - 6. The average Dirac point in this collection of devices is 21.78 V ± 2.67 V (Figure 4) and the average hole mobility is 4945 $cm^2/V*s$ ± 2000 $cm^2/V*s$ in ambient (Figure 5), indicating very high quality graphene with minimal doping on SiO_2 which compares favorably to results demonstrated in the literature.[30,31] As shown in the resistance histogram (Figure 6), the average device resistance is 6085 Ω ± 1838 Ω. The variation in the resistance likely comes from small tears in the graphene film created during the transfer process and slight differences in the contact resistance at the graphene/metal interface. Functionalization chemistry and normalization algorithms

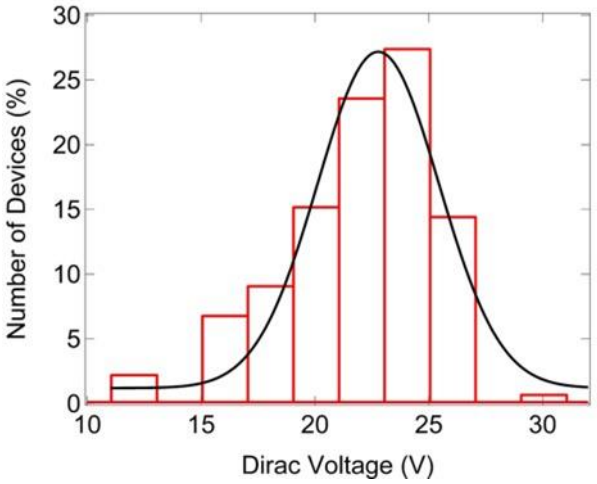

Figure 4: Histogram of Dirac voltage for more than 12,000 graphene transistors indicating low doping levels consistent with high quality graphene and reproducible fabrication methods.

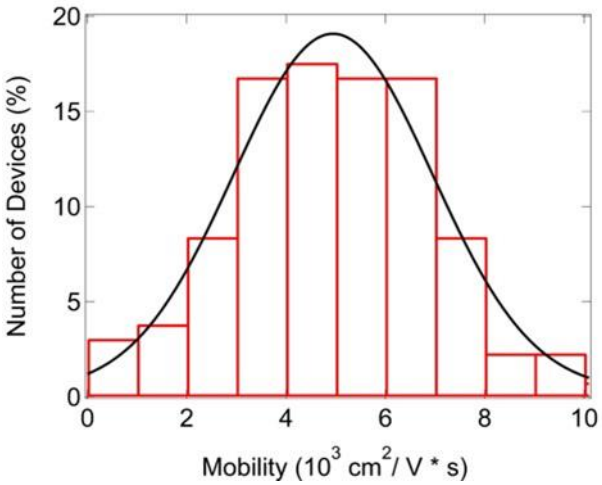

Figure 5: Histogram of hole mobility for over 12,000 graphene transistors. Over 90% of devices have mobility greater than 2000 $cm^2/V*s$, with an average mobility of nearly 5000 $cm^2/V*s$.

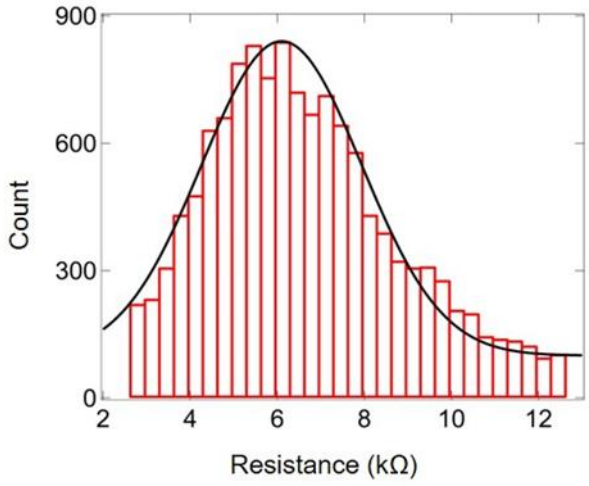

Figure 6: Resistance histogram for the same set of devices as Figures 4 - 5. Over 93% of transistors fall within a factor of 2 of 6 kΩ, a positive indication of the reproducibility of the fabrication techniques.

employed during data analysis are sufficiently robust to accommodate for this minimal level of device variation.

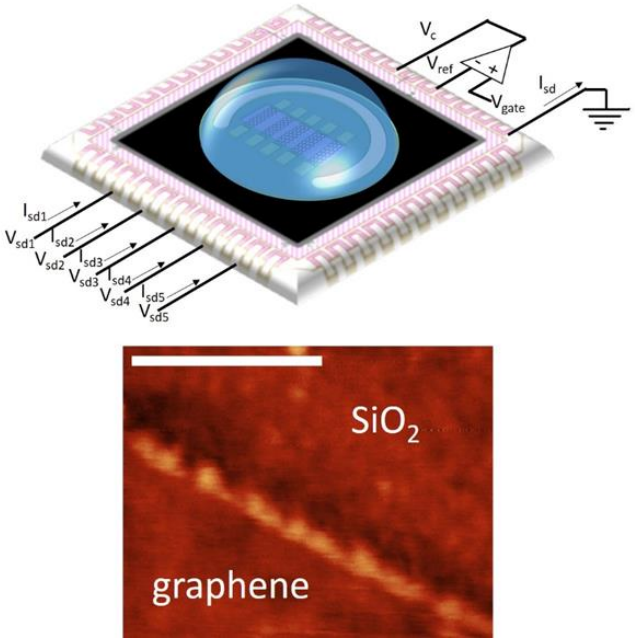

Figure 7: Graphene liquid gate schematic including readout circuit diagram with AFM image of the pristine graphene/SiO_2 interface. The AFM demonstrates the cleanliness of the surface prior to functionalization with an RMS roughness less than 0.3 nm. Graphene height is 0.7 nm above the SiO_2, consistent with previous reports.[14,15] Scale bar in the AFM image is 0.5 µm and Z scale is 7 nm.

Graphene FET Liquid Gating

The three terminal liquid gated graphene FET is exquisitely sensitive to fluctuations in the charge profile at the graphene-liquid interface, which lends this modality a high aptitude for sensing charged biomolecules and their dynamics.[23,24] The biosensing measurement is comprised of a voltage sweep by the immersed Pt reference electrode while measuring the source-drain current of the graphene channel. The contact area between the ionic liquid and Pt electrode is much larger than the area between the ionic liquid and the graphene layer, so the contribution to the total capacitance is dominated by the double layer of charge that forms at the graphene/liquid interface. Thus the gate voltage is effectively applied at the top gate, as has been well established in the literature.[32] The ionic, conductive liquid forms a double layer capacitance at the graphene-liquid interface, and this capacitive coupling alters the Fermi level in the graphene causing a shift in the current-gate voltage characteristic.[33] A schematic of graphene liquid gating is presented in Figure 7 along with an atomic force microscopy (AFM) image of contamination-free graphene, validating the cleanliness of the fabrication and packaging process.

Figure 8 is a plot of the charge transport properties of one of our liquid gated graphene devices at subsequent functionalization steps. The presence of a layer of charged

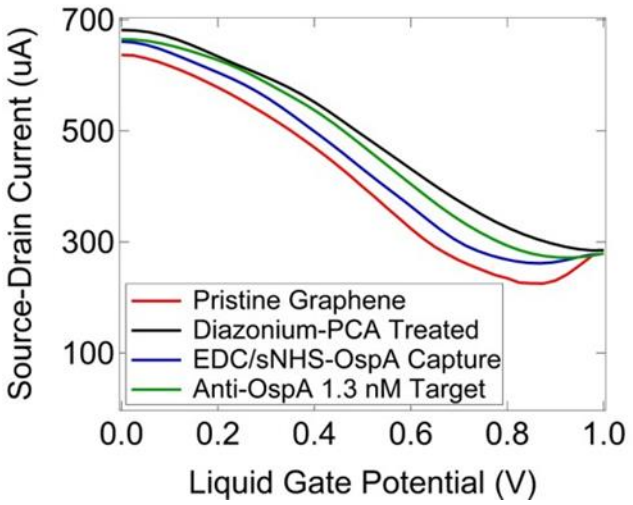

Figure 8: Liquid gated I-Vg at several functionalization steps. Note that the Dirac point is now closer to 0 V and the whole trace is generally condensed laterally relative to the data in Figure 4. This is due to the field effect of the double layer capacitance from the liquid being in much closer proximity to the graphene, hence less voltage is required to induce comparable shifts in the charge transport. The trace shifts between chemistry steps due to local gating effects at the graphene-liquid interface.[34]

capture biomolecules at this interface introduces a competing gating effect, shifting the pristine graphene curve to higher or lower gate voltages as shown in Figure 8. The eventual introduction of a target species that binds to the layer of capture molecules induces a conformational change in the layer of biomolecules, thus again shifting the electrostatic profile presented to the graphene layer and changing its charge transport properties in a manner characteristic of the target.[14,15] The direction and magnitude of these shifts in the plot of source-drain current versus liquid gate potential allow for highly sensitive and specific detection and quantification of target compounds.[10,15]

Several chemistry steps are employed to functionalize the graphene devices for use as biosensors. At each step, devices are characterized electronically and optically to ensure high performance. Carboxylic acid anchor sites for biomolecule binding are built on the graphene channels using covalent diazonium chemistry (4-carboxybenzene diazonium tetrafluoroborate synthesized in house) and noncovalent pyrene chemistry (TCI Item #P1687).[15,35] Thecarboxylic acid moieties are stabilized and activated with carbodiimide crosslinking chemistry (EDC/sulfo-NHS) (Amresco Item #N195/G Biosciences Item #BC97) and the capture molecule is bound to the graphene by a primary amine at the capture molecule surface, such as in a lysine residue. Blocking and quench steps (Broadpharm Item #BP-22355 and Alfa Aesar Cat# L14322) minimize nonspecific interactions in the graphene sensors.[36] The results of these chemical processes on the electronic transport characteristics indicate successful chemical functionalization as demonstrated in previous literature.[15]

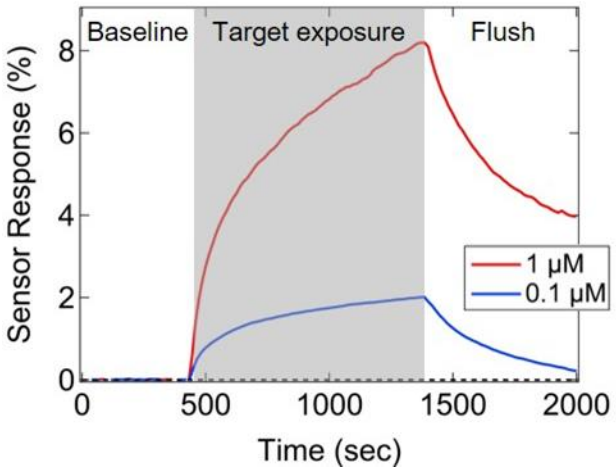

Figure 9: Normalized percentage change from baseline for the graphene source-drain current over time as two concentrations of GAP are introduced to Rho GTPase in the presence of GTP. Target GAP is added at 450 s and washed away at 1400 s causing a return to baseline.

Specifically, shifts in the Dirac voltage and reduction of the mobility, are evident in Figure 8 during the binding of MBP-tagged OspA protein (Rockland Cat #000-001-C13) to its antibody (Bioss Cat #bs-12879R). OspA is a biomarker antigen for Lyme disease, an autoinflammatory disease caused by bacterial infection that may lead to facial paralysis and seizures if left untreated.[37]The graphene sensor responds to OspA antibodies at a concentration of 1.3 nM as evidenced by a shift in the minimum conductance point and the slope of the I-Vg characteristic (blue to green lines) in Figure 8.

Biosensing with Functionalized Graphene Transistors

Figure 9 depicts the graphene sensor response when functionalized with Rho GTPase (a generous gift from Dr. Oegema at UCSD), a protein involved in intracellular actin dynamics, organelle development, and cell movement.[38] Wild type Rho GTPase catalyzes the conversion of GTP to GDP only in the presence of the GAP protein, which controls the rate of movement from the active to inactive conformation. At 450 seconds, the GAP protein is introduced (a generous gift from Dr. Oegema at UCSD) to the bound Rho GTPase on the graphene surface. The change in the graphene source drain current describes the conformational change of the Rho GTPase as physically binds the GAP. At 1400 seconds, the GTP/GAP-containing solution is washed off and replaced with buffer and the reaction shifts from products to reactants. The association and dissociation rates of the Rho GTPase for binding GAP are calculated using the equations describing a reversible binding reaction at equilibrium where molecule A binds to molecule B to form complex AB at the sensor surface.[39] We calculate an equilibrium dissociation constant K_D of 5.4 µM ± 0.4 µM for this interaction, which is in excellent agreement with the literature value of K_D for this protein and small molecule interaction of 3.95 µM.[40]

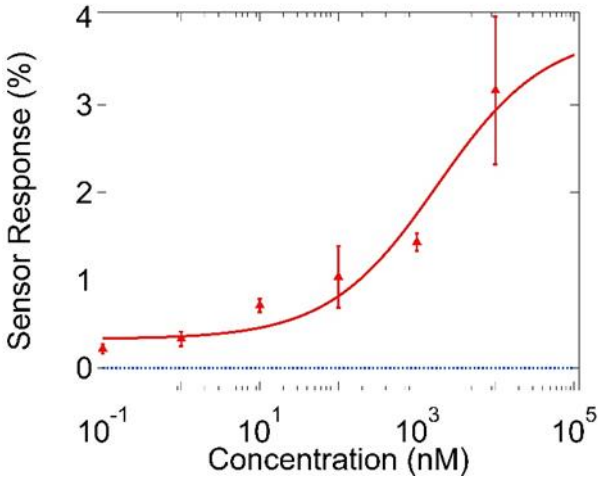

Figure 10: Standard curve of insulin binding to anti-insulin in serum. Sensing response (red points fit by red solid line) is differentiable from the buffer response (blue dotted line) in the pM regime.

Similar to an ELISA, the technology can be used to quantify the concentration of a target molecule in a sample against a standard curve to determine the limit of detection and binding affinity. The graphene linking chemistry is biomolecule-agnostic, it can work equally well for detection of small molecules, peptides, proteins, cells, viruses and other charged biomolecular species.[10] Further, due to the effective blocking chemistry, non-targeted species are ignored by the sensor; thus the sensors perform well in complex media such as whole blood, blood serum, various buffers, and cell growth media. In Figure 10, the sensor is functionalized with anti-insulin antibodies (LSBio Cat #LS-B3297) and sensor responses to insulin (LS Bio Cat #LS-G4582) in 1:10 diluted serum (Gibco Cat # 31053-028) are fit to the Hill-Langmuir function.[41] Insulin is an important hormone made by the pancreas that allows the body to use glucose from carbohydrates in food for energy. Notably, the empirically observed lower limit of detection where the sensing response was statistically differentiable from buffer (100 pM) and binding affinity constant K_D (1.8 µM) cover the clinically relevant regime which has far-reaching implications for the monitoring and treatment of diabetes.[42,43]

CONCLUSIONS

In summary, we developed a robust and reproducible graphene-enabled biosensor chip and corresponding readout infrastructure for measuring biomolecular interaction kinetics that exhibits excellent sensitivity down to pM levels, selectivity as it can function in complex media, and versatility in the myriad of target molecules that can be detected. Characterization of the graphene FETs demonstrate high carrier mobility and low defect density across thousands of samples. After functionalizing the graphene with diverse capture molecules of interest, device responses were shown to vary systematically with target molecule concentration in clinically relevant regimes. This technology can be used for investigating binding kinetics of antibody and antigen pairs or small molecule

binding for pharmaceutical assay development, comparable to a surface plasmon resonance (SPR) or biolayer interferometry tool (BLI) while using less reagents and less time to obtain data and providing a more efficient user experience. More explicitly, the Agile platform requires as little as 10 µL compared to 200 µL for a high end BLI tool and begins collecting kinetics data 5 minutes after sample preparation compared to over 3 hours from sample preparation on a common SPR tool all at an order of magnitude lower cost. Additionally, sample quantification can be performed akin to an ELISA measurement with all data collection and analysis requiring less than one day from start to finish, ushering in a new era of dynamic protein characterization enabled by nanotechnology. Large scale manufacturing and supply chain have been realized, moving this technology from the realm of promising candidate to available commercial product.

REFERENCES

1. Verkaik NJ, de Vogel CP, van Wamel WJB, van Belkum A. Bead-Based Flow-Cytometry in Medical Microbiological Research and Diagnosis. In: Hayes JP, Van Leeuwen WB, eds. *The Role of New Technologies in Medical Microbiological Research and Diagnosis*. ; 2012:151-160. doi:10.2174/978160805316211201010151.
2. Schmitz JL. Serologic Testing for Infectious Diseases. In: O'Gorman MRG, Donnenberg AD, eds. *Handbook of Human Immunology*. Second Edi. Boca Raton, FL: CRC Press; 2008:640.
3. Engvall E, Perlmann P. Enzyme-linked immunosorbent assay (ELISA) quantitative assay of immunoglobulin G. *Immunochemistry*. 1971;8(9):871-874. doi:10.1016/0019-2791(71)90454-X.
4. Berg JM, Tymoczko JL, Stryer L, eds. Immunology Provides Important Techniques with Which to Investigate Proteins. In: *Biochemistry*. Vol New York. Fifth Edit. ; 2002:320-323.
5. *ELISA Assay Trends*. Cambridge, UK; 2012.
6. Committee on Lyme Disease and Other Tick-Borne Diseases. Diagnostics and Diagnosis. In: *Critical Needs and Gaps in Understanding Prevention , Amelioration , and Resolution of Lyme and Other Tick-Borne Diseases: The Short-Term and Long-Term Outcomes*. Washington DC: National Academies Press (US); 2011:1-520.
7. Geim AK, Novoselov KS. The rise of graphene. *Nat Mater*. 2007;6(3):183-191. doi:10.1038/nmat1849.
8. Novoselov KS, Geim AK, Morozov S V, et al. Electric field effect in atomically thin carbon films. *Science (80-)*. 2004;306(5696):666-669. doi:10.1126/science.1102896.
9. Schwierz F. Graphene transistors. *Nat Nanotechnol*. 2010;5(7):487-496. doi:10.1038/nnano.2010.89.
10. Zhan B, Li C, Yang J, Jenkins G, Huang W, Dong X. Graphene field-effect transistor and its application for electronic sensing. *Small*. 2014;10(20):4042-4065. doi:10.1002/smll.201400463.
11. Zhu SE, Krishna Ghatkesar M, Zhang C, Janssen GCAM. Graphene based piezoresistive pressure sensor. *Appl Phys Lett*. 2013;102(16). doi:10.1063/1.4802799.
12. Esfandiar A, Kybert NJ, Dattoli EN, et al. DNA-decorated graphene nanomesh for detection of chemical vapors. *Appl Phys Lett*. 2013;103(18). doi:10.1063/1.4827811.
13. Lu Y, Goldsmith BR, Kybert NJ, Johnson ATC. DNA-decorated graphene chemical sensors. *Appl Phys Lett*. 2010;97(8). doi:10.1063/1.3483128.
14. Lu Y, Lerner MB, John Qi Z, et al. Graphene-protein bioelectronic devices with wavelength-dependent photoresponse. *Appl Phys Lett*. 2012;100(3). doi:10.1063/1.3678024.
15. Lerner MB, Matsunaga F, Han GH, et al. Scalable production of highly sensitive nanosensors based on graphene functionalized with a designed G protein-coupled receptor. *Nano Lett*. 2014;14(5):2709-2714. doi:10.1021/nl5006349.
16. Li Y, Chopra N. Progress in Large-Scale Production of Graphene. Part 1: Chemical Methods. *JOM*. 2015;67(1):34-43. doi:10.1007/s11837-014-1236-0.
17. Chen X, Zhang L, Chen S. Large area CVD growth of graphene. *Synth Met*. 2015;210:95-108. doi:10.1016/j.synthmet.2015.07.005.
18. Bae S, Kim H, Lee Y, et al. Roll-to-roll production of 30-inch graphene films for transparent electrodes. *Nat Nanotechnol*. 2010;5(8):574-578. doi:10.1038/nnano.2010.132.
19. Yan S. This bendable smartphone comes with a catch. *CNN Money*. May 2016.
20. Kobayashi T, Bando M, Kimura N, et al. Production of a 100-m-long high-quality graphene transparent conductive film by roll-to-roll chemical vapor deposition and transfer process. *Appl Phys Lett*. 2013;102(2). doi:10.1063/1.4776707.
21. Kang J, Shin D, Bae S, Hong BH. Graphene transfer: key for applications. *Nanoscale*. 2012;4:5527-5537. doi:10.1039/c2nr31317k.
22. Kim SJ, Choi T, Lee B, et al. Ultraclean Patterned Transfer of Single-Layer Graphene by Recyclable Pressure Sensitive Adhesive Films. *Nano Lett*. 2015;15(5):3236-3240. doi:10.1021/acs.nanolett.5b00440.
23. Vieira NCS, Borme J, Machado Jr. G, et al. Graphene field-effect transistor array with integrated electrolytic gates scaled to 200 mm. *J Phys Condens Matter*. 2016;28(8). doi:10.1088/0953-8984/28/8/085302.
24. Mackin C, Palacios T. Large-scale sensor systems based on graphene electrolyte-gated field-effect transistors. *Analyst*. 2016. doi:10.1039/c5an02328a.
25. Qvit N, Disatnik M-H, Sho J, Mochly-Rosen D. Selective phosphorylation inhibitor of δPKC-PDK protein-protein interactions; application for myocardial injury in vivo. *J Am Chem Soc*. 2016:jacs.6b02724. doi:10.1021/jacs.6b02724.
26. Novoselov KS, Fal'ko VI, Colombo L, Gellert PR, Schwab MG, Kim K. A roadmap for graphene. *Nature*. 2012;490(7419):192-200. doi:10.1038/nature11458.
27. Geim AK. Graphene: status and prospects. *Science*. 2009;324(5934):1530-1534. doi:10.1126/science.1158877.
28. Kybert NJ, Han GH, Lerner MB, Dattoli EN, Esfandiar A, Charlie Johnson AT. Scalable arrays of chemical vapor sensors based on DNA-decorated graphene. *Nano Res*. 2014;7(1):95-103. doi:10.1007/s12274-013-0376-9.
29. Gao L, Ren W, Xu H, et al. Repeated growth and bubbling transfer of graphene with millimetre-size single-crystal grains using platinum. *Nat Commun*. 2012;3:699. doi:10.1038/ncomms1702.
30. Li X, Cai W, An J, et al. Large-area synthesis of high-quality and uniform graphene films on copper foils. *Science (80-)*. 2009;324(5932):1312-1314. doi:10.1126/science.1171245.

31. Kumar S, Peltekis N, Lee K, Kim H-Y, Duesberg GS. Reliable processing of graphene using metal etchmasks. *Nanoscale Res Lett*. 2011;6(1):390. doi:10.1186/1556-276X-6-390.
32. Uesugi E, Goto H, Eguchi R, Fujiwara A, Kubozono Y. Electric double-layer capacitance between an ionic liquid and few-layer graphene. *Sci Rep*. 2013;3:1595. doi:10.1038/srep01595.
33. Xia J, Chen F, Li J, Tao N. Measurement of the quantum capacitance of graphene. *Nat Nanotechnol*. 2009;4(8):505-509. doi:10.1038/nnano.2009.177.
34. Lerner MB, Resczenski JM, Amin A, Johnson RR, Goldsmith JI, Johnson ATC. Toward quantifying the electrostatic transduction mechanism in carbon nanotube molecular sensors. *J Am Chem Soc*. 2012;134(35):14318-14321. doi:10.1021/ja306363v.
35. Choi Y, Olsen TJ, Sims PC, et al. Dissecting single-molecule signal transduction in carbon nanotube circuits with protein engineering. *Nano Lett*. 2013;13(2):625-631. doi:10.1021/nl304209p.
36. Huang Y, Dong X, Liu Y, Li L-J, Chen P. Graphene-based biosensors for detection of bacteria and their metabolic activities. *J Mater Chem*. 2011;21(33):12358. doi:10.1039/c1jm11436k.
37. Dunn JJ, Lade BN, Barbour AG. Outer surface protein a (OspA) from the lyme disease spirochete, borrelia burgdorferi: High level expression and purification of a soluble recombinant form of OspA. *Protein Expr Purif*. 1990;1(2):159-168. doi:10.1016/1046-5928(90)90011-M.
38. Zhang B, Zheng Y. Regulation of RhoA GTP Hydrolysis by the GTPase-Activating Proteins p190, p50RhoGAP, Bcr, and 3BP-1. *Biochemistry*. 1998;37(15):5249-5257.
39. de Mol NJ, Fischer MJE. Chapter 5. Kinetic and Thermodynamic Analysis of Ligand–Receptor Interactions: SPR Applications in Drug Development. In: *Handbook of Surface Plasmon Resonance*. Cambridge: Royal Society of Chemistry; 2008:123-172. doi:10.1039/9781847558220-00123.
40. Schonegg S, Constantinescu AT, Hoege C, Hyman AA. The Rho GTPase-activating proteins RGA-3 and RGA-4 are required to set the initial size of PAR domains in Caenorhabditis elegans one-cell embryos. *Proc Natl Acad Sci U S A*. 2007;104(38):14976-14981. doi:10.1073/pnas.0706941104.
41. Weiss JN. The Hill equation revisited: uses and misuses. *FASEB J*. 1997;11(11):835-841.
42. *Insulin ECLIA Assay*. doi:Catalog #12017547122.
43. Buse J, Polonsky K, Burant C. Type 2 diabetes mellitus. In: Melmed S, Polonsky K, Larsen P, Kronenberg H, eds. *Williams Textbook of Endocrinology*. 12th Editi. Philadelphia, PA: Elsevier; 2011.